Time evolution of thermodynamic entropy for conservative and dissipative chaotic maps

M. Baranger[a], V. Latora[b] and A. Rapisarda[b]
[a] *Center for Theoretical Physics, Laboratory for Nuclear Sciences and Department of Physics, Massachusetts Institute of Technology, Cambridge, Massachusetts 02139, USA*
[b] *Dipartimento di Fisica e Astronomia Universitá di Catania and INFN sezione di Catania, Corso Italia 57, I-95129 Catania, Italy*
(July 13, 2011)

We consider several low–dimensional chaotic maps started in far-from-equilibrium initial conditions and we study the process of relaxation to equilibrium. In the case of conservative maps the Boltzmann-Gibbs entropy S(t) increases linearly in time with a slope equal to the Kolmogorov-Sinai entropy rate. The same result is obtained also for a simple case of dissipative system, the logistic map, when considered in the chaotic regime. A very interesting results is found at the chaos threshold. In this case, the usual Boltzmann-Gibbs is not appropriate and in order to have a linear increase, as for the chaotic case, we need to use the generalized q-dependent Tsallis entropy $S_q(t)$ with a particular value of a q different from 1 (when q=1 the generalized entropy reduces to the Boltzmann-Gibbs). The entropic index q appears to be characteristic of the dynamical system.

I. INTRODUCTION

In this paper we study the connection between two quantities, both called entropies and used in two different fields: the entropy of a thermodynamic system S (the entropy of Boltzmann and Clausius, the entropy of the second law of thermodynamics) [1], and κ, the Kolmogorov–Sinai entropy, defined by the mathematicians as a measure of chaos and describing the dynamical instabilities of trajectories in the phase space [2,3]. As a main difference the thermodynamic entropy is a function of time, depending not only on the particular dynamical system, but also on the choice of an initial probability distribution for the state of that system, while κ is a single number, a property solely of the chaotic dynamical system considered. Moreover, the Kolmogorov–Sinai entropy it is not really an entropy but an entropy–rate, i.e. an entropy per unit time.

The connection between these two quantities has not been addressed extensively in the literature. Only few and often very vague statements are present in the textbooks [4]. Though some similar ideas have appeared previously in the literature [5,6], a clarification of this connection has been proposed for strongly chaotic hamiltonian systems by two of the authors in ref. [7].

Here we consider conservative and non–conservative chaotic systems. We focus in particular on two two–dimensional conservative maps, the cat and the standard map, and on the logistic map, the simplest one–dimensional dissipative system. We start the system in far–from–equilibrium initial conditions, and we follow numerically the process of relaxation to equilibrium. When the dynamics is chaotic the variation with time of the physical entropy goes through three successive, roughly separated stages. In the first one, $S(t)$ is dependent on the details of the dynamical system and of the initial distribution, and no generic statement can be made. In the second stage, $S(t)$ is a linear increasing function of time. In the third stage, $S(t)$ tends asymptotically towards the constant value which characterizes equilibrium, for which the distribution is uniform in the available part of phase space. The actual connection requires $S(t)$ to be averaged over many histories, so as to give equal weights to initial distributions from all regions of phase space. When such average is performed a perfect equality $dS/dt = \kappa$ is obtained in the intermediate stage.

In this paper we also address a very special situation, i.e. the case of the logistic map at the edge of chaos. It has been shown that in order to be treated such a special border of chaos situation requires the nonextensive definition of entropy $S_q(t)$ [8].

II. CONSERVATIVE CHAOTIC SYSTEMS

As a first example we consider the "generalized cat map", defined by the following iterative rule inside a unit square:

$$\begin{aligned} P &= p + aq \qquad (\mathrm{mod}\ 1) \\ Q &= p + (1+a)q \qquad (\mathrm{mod}\ 1) \end{aligned} \tag{1}$$

where a is a positive control parameter. In fig. 1 we consider an initial distribution very strongly localized in a tiny region of the phase space, and we let it evolve in time according to the eqs. (1) with $a = 1$. The distribution stretches in one direction and contracts in another. The volume of the distribution in phase space is conserved because of the Liouville's theorem, while its shape keeps changing in time until the system reaches a stationary state with an uniform filling of the phase space.

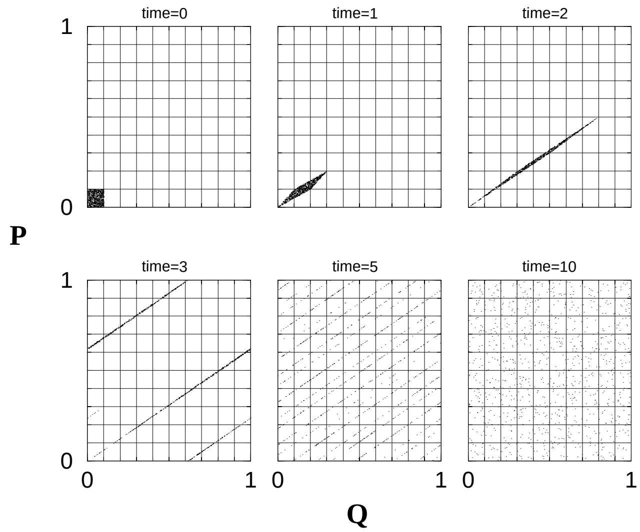

FIG. 1. Generalized Cat Map with $a = 1$. Time evolution of an initial distribution of points; we report the following time steps 0,1,2,3,5,10.

Any fine–grained quantity (for example an entropy defined as an integral over the phase space) does not vary with time at all. However the shape of the volume becomes increasingly complicated due to the chaotic dynamics. In order to have an entropy which is increasing in time (in agreement with the second principle of thermodynamics) we simply need to perform a coarse–graining, i.e. a slight smearing, or smoothing, of the probability distribution in phase space before calculating S [9]. There are many ways to introduce a coarse–graining. In this paper, we assume that phase space is divided into a grid of a large number M of cells c_i with volumes v_i, such that $\sum_i v_i = V$, the total volume of available phase space. In fig. 1 we report a grid of M = 10x10 cells, though for the actual calculations of this paper we will use a much more refined coarse–graining. Our definition for the out–of–equilibrium entropy is then the coarse–grained Boltzmann-Gibbs entropy:

$$S(t) = -\sum_i \; p_i(t) \; \log p_i(t) \quad , \tag{2}$$

where $p_i(t)$ is the probability that the state of the system falls inside cell c_i of phase space at time t. Such a coarse–grained entropy is a quantity which is increasing in time, and the chaotic dynamics is the main reason of this increase. In the following of this paper we will show the fundamental importance of chaos in the relaxation to equilibrium: the entropy increases with a rate exactly equal to the Kolmogorov–Sinai entropy, the measure of chaos. N.S.Krylov, already in the 1940's [10], was the first one who understood clearly that the *mixing* property of chaos was essential for the foundations of statistical mechanics. In fig. 2 we show $S(t)$ for four values of a (see caption). Now the coarse–graining grid is obtained by dividing each axis into 400 equal segments. The initial distribution consists of 10^6 points placed at random inside a square whose size is that of a coarse–graining cell, and the center of that square is picked at random anywhere on the map. In this way the initial distribution is very strongly localized in phase space i.e. all the cells but a few contain initial zero probability.

Each of the four curves is an average over 100 runs, i.e. 100 histories with different initial distributions chosen at random, as mentioned. Each curve shows clearly the stage–2 linear behavior, the slope dS/dt being accurately given by the KS entropy–rate κ. To calculate κ here, we have used the fact that it is equal to the sum of the positive Lyapunov exponents [11]. In the case of cat map we have only one positive analytically calculable Lyapunov exponent λ, given by the equation:

$$\kappa = \lambda = \log \frac{1}{2}(2 + a + \sqrt{a^2 + 4a}) \quad . \tag{3}$$

The values of κ are reported in the figure caption.

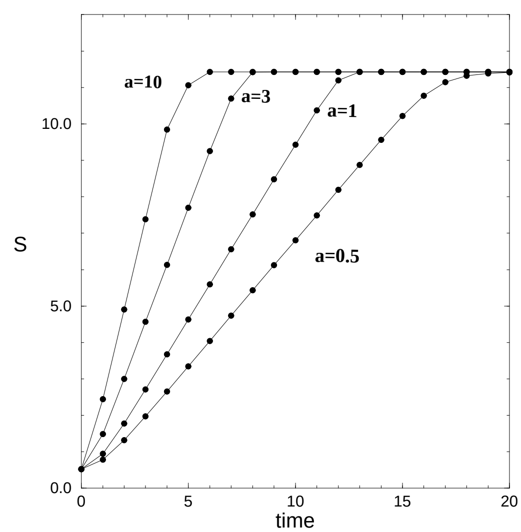

FIG. 2. We show the thermodynamical entropy S vs time for the Generalized Cat Map, with $a = 10, 3, 1, 0.5$. We considered $N = 10^6$, grid $= 400\times400$, $V_i = V_{\rm cell}$, and an average of 100 histories. The slope of the linear rise coincides with the Kolmogorov-Sinai entropy which is $\kappa = 2.48, 1.57, 0.96, 0.69$ respectively from right to left. See text for more details.

The equality $dS/dt = \kappa$ is valid in the intermediate stage for each of the four a values considered in figure. Moreover it can be shown that this result does not depend on the size of the initial distribution and on the size of the coarse–graining cells [7]. The type of coarse–graining we adopted allows an alternative version of the significance of κ for the evolution of a physical system. Starting from an initial distribution localized in phase space (like in fig.1), during the generic second stage mentioned earlier, the total number of occupied cells, i.e. cells with non-vanishing p_i, varies proportionally to $e^{\kappa t}$. Our simulations verify this fact well [7].

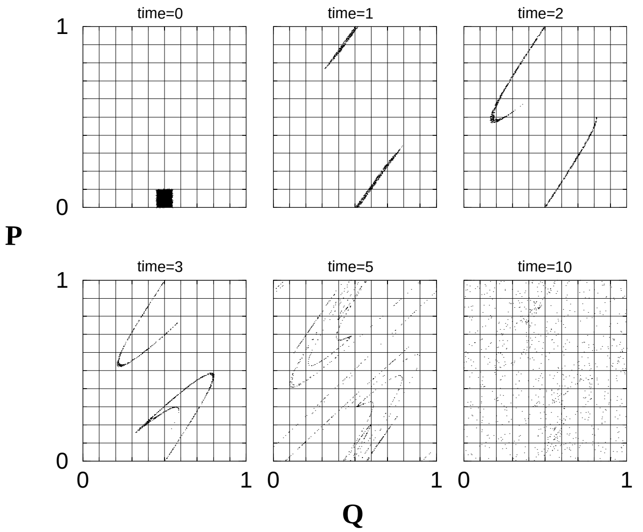

FIG. 3. Standard Map with $a = 5$. Time evolution of an initial distribution of points; we report time=0,1,2,3,5,10

The second system we have studied is the standard map [12], again a two-dimensional conservative map in the unit square, but this time nonlinear:

$$\begin{aligned} P &= p + \frac{a}{2\pi}\ \sin(2\pi q) \qquad (\text{mod } 1)\ , \\ Q &= q + P \qquad\qquad\qquad (\text{mod } 1)\ . \end{aligned} \tag{4}$$

The map is only partially chaotic, but the percentage of chaos increases with the control parameter a, and we consider large values of a, namely 20, 10, and 5. For $a = 5$ there are still two sizeable regular islands, associated with a period 2 stable trajectory while for $a = 10$ and $a = 20$ the phase space is completely chaotic. In fig. 3 we report for the case $a = 5$ the time evolution of an initial small distribution located in the chaotic region of the phase space. As a main difference with respect to fig. 1, is that for a nonlinear system the stretching and contraction rates and directions vary appreciably in the phase space from place to place. The distribution bends on itself many times, nevertheless at the final time the system tends to occupy the whole chaotic part of the phase space in an uniform way. Fig. 4 presents three single histories (full lines) for $a = 5$, as well as an average curve (circles) as in fig .2. The coarse–graining grid, the choice of initial distribution, and the averaging are the same used for the cat map, but it was necessary to include 1000 histories in order to obtain a good averaging. In fact, for a very nonlinear system as the standard map, the single curves can vary wildly and, differently from the case of the cat map, thus the averaging procedure is essential. Fig. 5 shows the final average curves $S(t)$ for three values a: the one at the bottom corresponds to the smallest one.

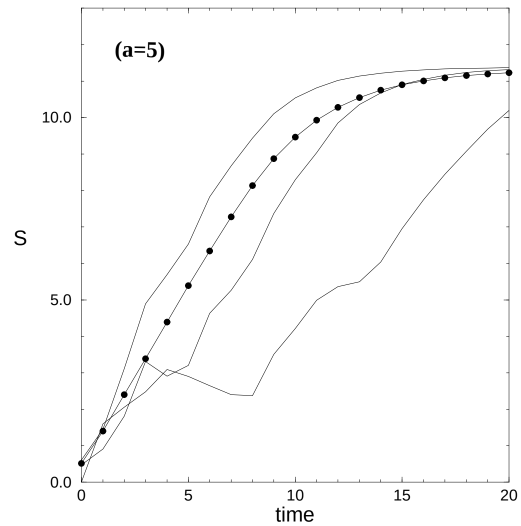

FIG. 4. The evolution of $S(t)$ for the Standard Map, with $k = 5$. Also in this case the linear slope of the average curve (full circles) corresponds to the Kolmogorov–Sinai entropy $\kappa = 0.98$. Three single histories (thin full lines) are compared with the average one calculated over 1000 histories. See text for further details.

We calculated numerically the Kolmogorov–Sinai entropy from the Lyapunov exponent, leaving out the regular islands for $a = 5$. This yielded $\kappa = \lambda = 0.98, 1.62, 2.30$, respectively for the three a's. Each curve has a stage–2 linear portion whose slope is correctly given by κ.

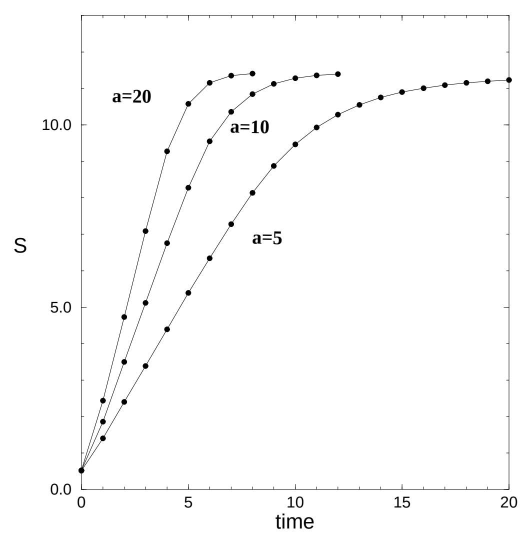

FIG. 5. The same as fig.2 for the Standard Map, $k = 20, 10, 5$ (from right to left). In this case the Kolmogorov–Sinai entropy is $\kappa = 2.30,\ 1.62,\ 0.98$ respectively. It was considered $N = 10^6$, grid $= 400 \times 400$, $V_i = V_{\text{cell}}$. An average of 100 trajectories was used for $k = 20, 10$, while 1000 histories were necessary for $k = 5$.

We return again to the need for averaging many histories starting from different parts of phase space. This has to be done whenever the local Lyapunov exponents varies appreciably from place to place, which is the normal case for nonlinear systems. For linear maps (like the generalized cat map below) it is not necessary. For other systems, it would never be necessary if we could use a fine–enough coarse–graining, to give the probability time to spread throughout phase space before any appreciable increase in entropy. Unfortunately such fine grain would require computers far more powerful than exist now. In the real thermodynamical world with many dimensions, what kind of coarse–graining should preferably be used is, we believe, a wide open question.

III. THE LOGISTIC MAP

We focus now on the dissipative case, and more specifically on the logistic map:

$$X = 1 - ax^2 \quad -1 \le x \le 1;\ 0 \le a \le 2; \tag{5}$$

Despite being an extremely simple one–dimensional equation, the logistic map has always been used as a paradigmatic example of non–conservative chaotic systems, because it inglobes all the fundamental characteristics of a non–conservative system. The logistic map shows different regimes, according to the value of the control parameter a [3]. In particular it is regular (negative Lyapunov exponent λ) for a smaller than a critical value $a_c = 1.401155198...$, and is chaotic for most part of the region $a > a_c$. At the chaos threshold $a = a_c = 1.401155198...$ the Lyapunov exponent vanishes and this is the famous *edge of chaos* situation [13]. Before moving to the study of the entropy time evolution we need to discuss first the problem of the sensitivity to initial conditions. For all the cases in which the Lyapunov exponent λ is positive we expect on the average an exponential increase of any small initial distance $\xi(t) \equiv \frac{x_t - x'_t}{x_0 - x'_0}$ to hold:

$$\xi(t) = \exp(\lambda t) \tag{6}$$

where x_t and x'_t are the position at time t of two initially close trajectories. This case will be referred in the following as *strongly sensitive* to the initial conditions. Instead at the edge of chaos $\lambda = 0$, and the following equation has been proven to be valid in ref. [14]

$$\xi(t) = [1 + (1-q)\lambda_q t]^{\frac{1}{1-q}} \quad (q \in \mathcal{R}) \tag{7}$$

which recovers Eq. (6) as the $q = 1$ particular case. The case $q < 1$ will be referred to as *weakly sensitive* to the initial conditions. So, *strong* and *weak* respectively stand for *exponential* and *power-law* time evolutions of $\xi(t)$. A *weakly sensitive* system is well described once q, i.e. the exponent of the power–law, is given. In particular at $a = a_c$ a value $q^* = 0.2445...$ is obtained [14].

We now apply to the logistic map the same kind of analysis used for conservative systems. The phase space interval $-1 \le x \le 1$ is partitioned into 10^5 equal cells c_i. The initial distribution consists of $N = 10^6$ points placed at random inside an interval picked at random anywhere on the phase space, and whose size is that of a cell. As the system evolves the probabilities $p_i(t)$ are computed at each time step.

In order to study in the same framework either the chaotic case and the edge of chaos situation we consider a generalized non–extensive entropy proposed a decade ago in ref. [17] as a physical starting point to generalize statistical mechanics and thermodynamic:

$$S_q(t) \equiv \frac{1 - \sum_i [p_i(t)]^q}{q-1} \quad (q \in \mathcal{R})\ . \tag{8}$$

This entropy is a function of the entropic index q and reduces to the Boltzmann-Gibbs entropy, defined in equation (2), when $q = 1$. A complete review of the existing theoretical, experimental and computational work about this entropy can be found in ref. [18]. In particular it has been shown that such an entropy covers some types of anomalies due to a possible multifractal structure of the relevant phase space. For example, whenever we have long-range interactions [19], long-range microscopic memory [20], or multifractal boundary conditions [14].

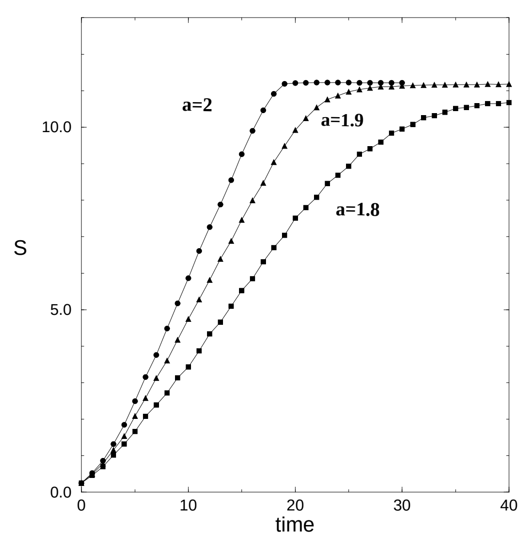

FIG. 6. We show for the logistic map the time evolution of S for the following values of a: $a = 2$, $a = 1.9$ and $a = 1.8$; The curves are averages of 500 histories. The slopes of the curves in the linear regime are equal to the corresponding Lyapunov exponents. See text.

We discuss in the rest of the paper the following results obtained for the logistic map [8]:

1) In the chaotic regime $q = 1$: the Boltzmann-Gibbs entropy 2 exhibits a linear increase in time, and the rate of increase is equal to κ.
2) The standard Boltzmann-Gibbs entropy is inadequate to describe the edge of chaos situation. Instead it is the non–extensive entropy which grows linearly with time for a particular value $q \neq 1$.

A. The chaotic case

In fig. 6 we present our results for the logistic map in correspondence of three values for a, all of them in the chaotic regime, namely $a = 2, 1.9, 1.8$. Fluctuations are of course present (as t increases), though their numerical importance can be cancelled by considering averages on the initial conditions. Each of the curves is an average over 500 runs, i.e., 500 histories with different initial distributions chosen at random, as mentioned. Though the asymptotic value, corresponding to a smooth distribution in the available part of phase space, is different in the three cases, all the curves show a linear increase on entropy. The slope in the intermediate time stage does not depend on the dimension of the cells and on the distribution size [8] and is equal to the predicted Lyapunov exponent, respectively $\ln 2$, 0.61 and 0.48 . Therefore the same results found for conservative maps hold also for the logistic map, though the latter is a nonconservative one.

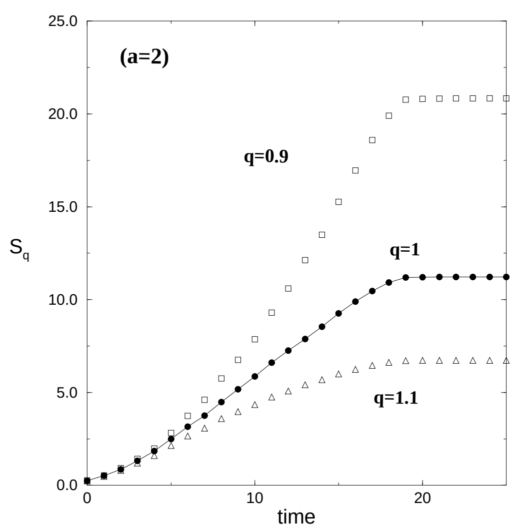

FIG. 7. For the logistic map with $a = 2$, we draw the time evolution of the non–extensive entropy S_q, considering three different values of q. Results are averages over 500 histories. See text for further details.

In fig. 7 we focus on the case $a = 2$ and instead of $S(t)$ we consider the time evolution of S_q, as defined by eq. 8, for three different values of q . As t evolves, $S_q(t)$ tends to increase (in all cases bounded by $\frac{M^{1-q}-1}{1-q}$, or $\ln M$ when $q = 1$). Only the curve for $q = 1$ shows a clear linear behavior and the slope is equal to the Lyapunov exponent $\ln 2$. For $q < 1$ the curve is concave, while for $q > 1$ the curve is convex. Therefore for the logistic map in the chaotic regime the standard Boltzmann–Gibbs must be used as for any hamiltonian chaotic system or conservative map.

B. The edge of chaos

So far we have shown that q is 1 for all the cases in which the logistic curve is chaotic, i.e. strongly sensitive to the initial conditions. Now we want to study the same system at its chaos threshold, i.e. at $a = a_c \simeq 1.401155198...$ for which the Feigenbaum attractor exists. We expect in this case a particular value $q \neq 1$, due to the fractality of phase space [8] and power-law sensitivity to initial conditions. For such a value of a, much bigger fluctuations than in the chaotic case are observed. To understand this it is sufficient to consider that the attractor occupies only a tiny part of phase space (844 cells out of the 10^5 of our partition). We therefore require a very efficient and careful averaging over the initial conditions. Here we adopt a selection method of the best histories based on how good is each initial condition at spreading itself. We obtain 1251 histories and we address to ref. [8] for all the details about the selection method. In fig.8 we plot $S_q(t)$ for four different values of q ; the curves are an average over the 1251 histories selected. The growth of $S_q(t)$ is found to be linear when $q = q_c = 0.2445$, while for $q < q_c$ ($q > q_c$) the curve is concave (convex).

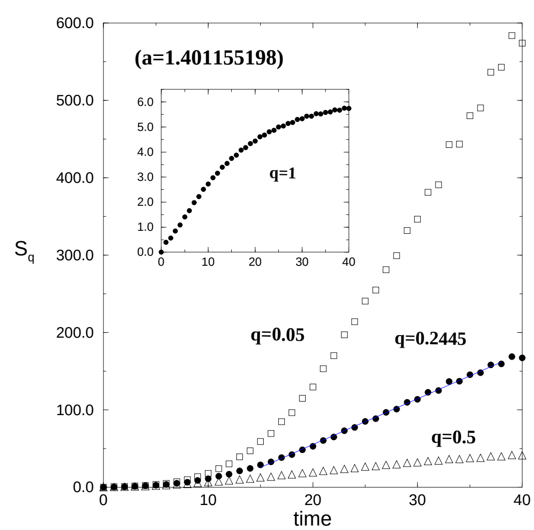

FIG. 8. Time evolution of S_q for $a = a_c$. We consider four different values of q . The case $q = 1$ is in the inset. Results are averages over 1251 histories.

This behavior is similar to the one in fig.7, with a major difference: *the linear growth is not at $q = 1$, (see inset in fig.8), but at $q = q_c = 0.2445$.* To extract the particular value of q for which we get the best linear rise of the nonextensive entropy, we have fitted the curves $S_q(t)$ in the time interval $[t_1, t_2]$ with the polynomial $S(t) = a + bt + ct^2$. We define the coefficient $R = |c|/b$ as a measure of the importance of the nonlinear term in the fit: if the points are on a perfect straight line, R should be zero. We choose $t_1 = 15$ and $t_2 = 38$ for all q's. Fig.9 shows that the minimum of $R = |c|/b$ occurs for $q = q_c = 0.2445$.

The value of q which allows for a linear growth of $S_q(t)$, obtained through this procedure, happens to coincide with the value q^* obtained in a completely different method by studying the power-law sensitivity to initial conditions [14].

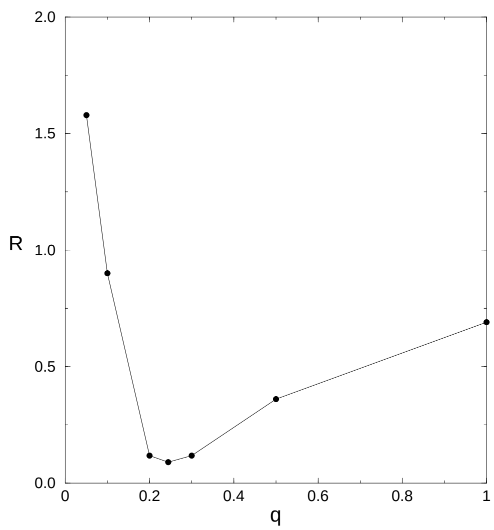

FIG. 9. Coefficient of nonlinearity R vs. q. See text for further details.

There exists also another method, based only on the geometrical description of the multifractal attractor existing at a_c, which gives exactly the same value of q [14]. The multifractal attractor can be characterized by using the multifractal function $f(\alpha)$ [3]. This function is defined in the interval $[\alpha_{min}, \alpha_{max}]$, and its maximum equals the fractal or Hausdorff dimension d_f. For a large class of systems the value of q can be calculated from

$$\frac{1}{1-q^*} = \frac{1}{\alpha_{min}} - \frac{1}{\alpha_{max}} \ , \qquad (9)$$

where α_{min} (α_{max}) is the lowest (highest) value for which $f(\alpha)$ is defined. In particular for the logistic map at the edge of chaos $\alpha_{min} = 0.380...$, $\alpha_{max} = 0.755...$ and $q^* = 0.2445$.

Finally, it is also interesting to note, that our result for the linear growth of S_q at the edge of chaos has been recently confirmed by using a different method [21].

IV. CONCLUSIONS

To summarize, we have illustrated, through several numerical examples for conservative and dissipative chaotic maps, the relationship existing between the Boltzmann equilibrium thermodynamic entropy S the Kolmogorov–Sinai one κ used for dynamical systems. As Krylov already suggested in the early '40s [10], the mixing property characteristic of chaos is fundamental in order to reach the thermodynamical equilibrium. When using a coarse-graining procedure, the growth of $S(t)$ averaged over many histories is linear and the slope gives just the Kolmogorov–Sinai entropy. This has been verified also for a dissipative case, i.e. the logistic map in the chaotic regime. Finally, a very interesting generalization must be done at the chaos threshold, where the sensitivity to initial conditions is not exponential, but power–law like. In this case, in fact, in order to have a linear growth for the entropy, as for the full chaotic regime, the non–extensive entropic form introduced by Tsallis should be adopted. The latter has been successfully checked for many cases where long–range correlations and a fractal phase space is found. We have shown that we get a linear growth for the generalized entropy only when the value $q = 0.2445$ (and not $q = 1$ for which the standard entropy is recovered) is used. This fact confirms previous numerical studies and generalizes the connection between the two entropies also at the edge of chaos. We conclude hoping that our results could stimulate a deeper undestanding of the connections between dynamics and statistical mechanics.

It is a pleasure to aknowledge the stimulating collaboration with Constantino Tsallis for the results on the logistic map.

[1] R. Balian, *From Microphysics to Macrophysics*, vol. I, Springer–Verlag, New York (1991).
[2] A. N. Kolmogorov, Dokl. Akad. Nauk SSSR **119**, 861 (1958); **124**, 754 (1959).
[3] C. Beck and F. Schlogl, *Thermodynamics of chaotic systems* (Cambridge University Press, Cambridge, 1993).
[4] One of the most explicit is on p. 39 of G. M. Zaslavsky, *Chaos in Dynamic Systems*, Harwood, Chur (1985).
[5] C.Dellago and H. A. Posch, Phys. Rev. E **55**, R9 (1997). This paper really treats two subjects; the second subject is the relevant one here.
[6] Y. Gu, J. Wang, Phys. Lett.A **229**, 208 (1997).
[7] V. Latora and M. Baranger, Phys. Rev. Lett. **82**, 520 (1999).
[8] V. Latora, M. Baranger, A. Rapisarda, C. Tsallis, to appear in Phys. Lett.A, cond-mat/9907412.
[9] R. Balian, *loc. cit.* p. 135.
[10] N.S.Krylov *Works on the Foundations of Statistical*

Physics, translated by A.B. Migdal, Ya. G. Sinai and Yu. L. Zeeman, Princeton University Press (1979).

[11] Ya. B. Pesin, Russian Math. Surveys **32:4**, 55 (1977).

[12] M. Tabor, sec. 4.2.e in *Chaos and Integrability in Nonlinear Dynamics*, Wiley, New York (1989).

[13] P.Bak, *How Nature Works : The Science of Self-Organized Criticality*, (Springer–Verlag, New York 1996); A. Bhowal, Physica A **247**, 327 (1997).

[14] U.M.S. Costa, M.L. Lyra, A.R. Plastino and C. Tsallis, Phys. Rev. E **56**, 245 (1997) and M.L. Lyra and C. Tsallis, Phys. Rev. Lett. **80**, 53 (1998).

[15] V. I. Arnold, *Mathematical Methods of Classical Mechanics*, Springer–Verlag, New York (1978).

[16] G. Benettin, L. Galgani, A. Giorgilli, and J.M. Strelcyn, Meccanica **9**, 21 (1980); A. Wolf, J. Swift, H. Swinney, and J. Vastano, Physica D **16**, 285 (1985).

[17] C. Tsallis, J. Stat. Phys. **52**, 479 (1988.

[18] C. Tsallis, in "Nonextensive Statistical Mechanics and Thermodynamics", eds. S.R.A. Salinas and C. Tsallis, Braz.
J. Phys. **29**, 1 (1999), Physics Today (2000) in press. [http://sbf.if.usp.br/WWW_pages/Journals/BJP/Vol29/Num1/index.htm].

[19] C. Anteneodo and C. Tsallis, Phys. Rev. Lett. **80**, 5313 (1998); V. Latora, A. Rapisarda and S. Ruffo, Phys. Rev. Lett. **83**, 2104 (1999), Physica D**131**, 38 (1999), and Phys. Rev. Lett. **80**, 692 (1998).

[20] M. Buiatti, P. Grigolini and L. Palatella, Physica A **268**, 214 (1999).

[21] S. Montangero, L. Fronzoni and P. Grigolini , cond-mat/9911412.